Development of Ka-Band Inflatable Layered-Lens Technology

L. R. Amaro,[1] S. Datthanasombat,[2] A. Prata, Jr.,[1,2] and J. A.Harrell[1]

This article documents the results of work performed at the Jet Propulsion Laboratory on layered-lens technology during 1999 and 2000. The main thrust of this effort was to demonstrate the feasibility of a three-layer lens for use with inflatable technology. A proof-of-concept unit was built and tested as a technology demonstration. Two proof-of-concept models were designed and tested at two different frequencies, 8.421 GHz (X-band) and 32.05 GHz (Ka-band). Both units produced adequate radiation characteristics, but slightly lower than the expected 50 percent efficiency (measured values of 41 percent and 33 percent, respectively). The results obtained show good potential, but further study is needed to improve performance.

I. Introduction

The function of a typical lens is to transform a spherical wave into a plane wave (in transmit mode). Lenses do this by selectively delaying portions of the incident spherical wave front radiated by a source in such a way that the emerging wave front is planar after passing through the lens. Most lenses achieve this by virtue of their physical shape and constitutive dielectric.

A layered lens performs this same function in a slightly different way. A layered lens uses multiple layers of conductive elements supported by a thin dielectric layer; each layer is separated by free space (see Fig. 1). These conducting elements form a space-fed array located on the surface of each layer. The dielectric layers do not contribute to the performance of the lens. The sole function of the dielectric layer is to provide the mechanical means to support the conducting elements. An incident electric field, E_i, illuminates the elements, which in turn re-radiate with a particular amplitude and phase determined by their dimensions. The transmitted field, E_t, is a composite of the incident field, E_i, and the field scattered by all the elements; by proper design, the transmitted field is a plane wave. Multiple layers are needed to provide the required 360-deg phase range in order to provide a plane wave on the emergent side and also minimize reflections from the lens. One layer alone cannot provide the full 360 deg of phase range and will scatter equally in the forward and reverse direction. Multiple layers yield the 360-deg phase range and can be adjusted to minimize the overall lens reflection by proper phasing of the reflection from each layer. To design the lens, a set of curves needs to be generated relating the element dimensions to

[1] Spacecraft Telecommunications Equipment Section.

[2] University of Southern California, Los Angeles.

The research described in this publication was carried out by the Jet Propulsion Laboratory, California Institute of Technology, under a contract with the National Aeronautics and Space Administration.

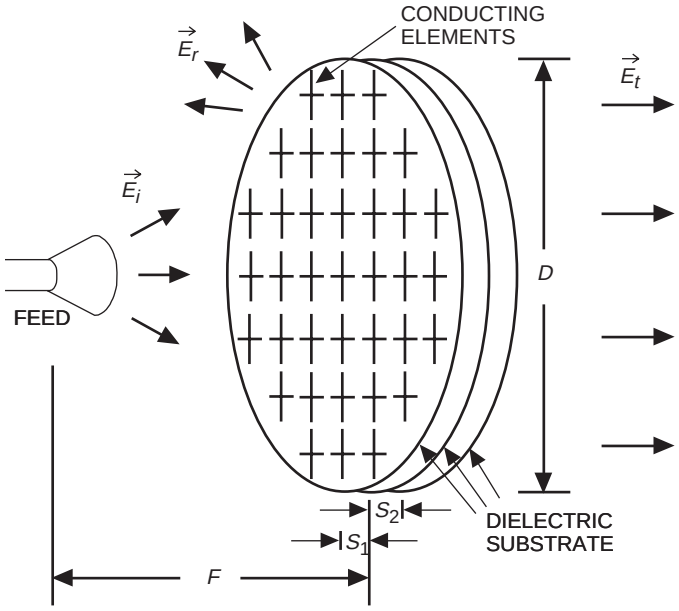

Fig. 1. Conceptual diagram of a layered lens showing related field quantities and pertinent features.

the electrical properties of the element (i.e., complex transmission coefficient, $T = E_i/E_r$). To obtain these curves, the element is analyzed in an infinite-array environment. The numerical modeling of the lens is done using a set of Fortran programs developed specially for this work. The analysis software is a method-of-moments-based integral equation solution of Maxwell's equations. The software is used to compute the field scattered by the elements. The dimensions and shapes of the elements are selected based on the required phase shift needed from each element. Elements of different sizes provide the required 0- to 360-deg phase range. The sizes of the elements change as one moves away from the center of the lens (reference phase); this is due to the feed-to-lens path-length increase. Therefore, to transform the spherical wave into a plane wave, a progressive phase shift is needed in the radial direction. As one moves outward from the lens axis, the phase varies from 0 to $N \times 360$ deg, where N is a negative integer.

Because the wave is impervious to the $N \times 360$ deg ambiguity (i.e., the wave cannot distinguish an $N - 1$ phase shift from an N phase shift), the dimensions of the elements will repeat every 360 electrical degrees. This effect can be seen as a radial "zoning" on the layers of the lens (see Fig. 2). Multiple layers can be used to increase the operational bandwidth and implement a dual-band lens, e.g., 8.421 GHz (X-band) and 32.05 GHz (Ka-band), and also to minimize the energy reflected by each layer. An earlier example of a layered lens was described by Robert Milne in 1982. His design used seven layers and operated at 5 GHz (C-band) [2]; this large number of layers does not stress the elements' radiation as a three-layer design would.

When compared with a reflector antenna, a lens antenna has a few advantages that at first are not obvious but are important to keep in mind: (1) As shown in Appendix A, a layered lens is almost an order of magnitude less sensitive to surface imperfections; (2) A layered-lens can be more easily stowed and deployed because of its low sensitivity to surface deformation; (3) It has no aperture blockage; and (4) Manufacture of a layered lens is relatively inexpensive, even in small quantities, because photolithography is a relatively inexpensive process. These four points make layered lenses a very desirable and convenient high-gain antenna candidate to implement with inflatable technology.

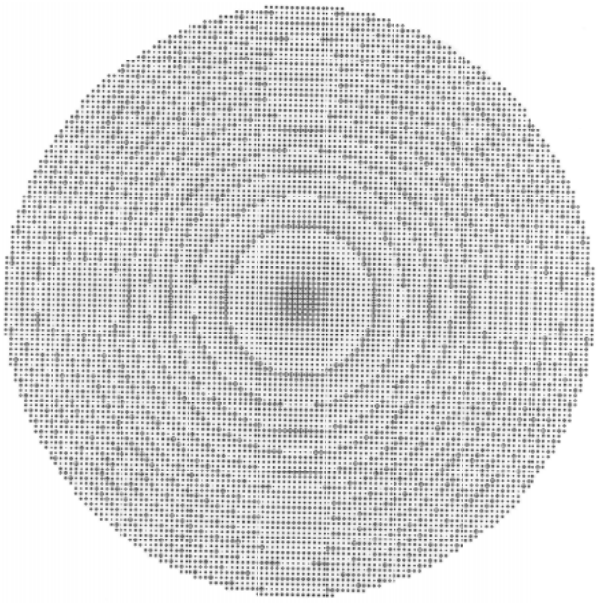

Fig. 2. Ka-band layered lens configuration (note the "zoning").

II. Demonstration Hardware Design and Development

The original proposed work called for the design, manufacture, and test of a 1-m-diameter layered lens. However, a 0.610-m-diameter (D in Fig. 1) size was chosen instead because it was the widest size that local vendors could etch. To further increase the size of the lens would require the layers to be made in strips and then pieced together. The assembly would require the strips to be precision aligned and supported, which could introduce alignment errors and support problems. The 39 percent reduction in diameter allowed us to demonstrate the feasibility of a layered-lens design without introducing errors that could not easily be accounted for. Along with the Ka-band lens, an X-band lens was also implemented to be used as a diagnostic tool if needed. The lenses were designed for an F/D of 0.5, which allows the use of a small feed horn with a 10-dB taper at 45-deg incidence on the rim elements. Three equal layers were used for the design. Two layers would have lower reflections since the reflection of each layer can be made to cancel each other. However, this would require an array element capable of producing large phase variations, and at present no such element is known.

The elements were chosen to have a worst-case transmission coefficient of 0.8 (a value of 1 equates to full transmission) at the design frequency; this value of transmission coefficient corresponds to a design efficiency of 60 percent. The 60 percent efficiency does not include ohmic or dielectric losses or manufacturing errors. Since the layered lens behaves as a space-fed array, the spacing between elements was chosen to ensure the absence of grating lobes (i.e., spacing $<\lambda_o$). Two small high-performance corrugated horns were designed and built specially for feeding the lens (see Fig. 3). These were designed to have very low cross-polarization isolation performance, $\geq$ 40 dB (witnin $\pm$45 deg of boresight), and low return loss, $\geq$ 34 dB, over the band of interest. Axial corrugations were used to facilitate machining. The excellent performance of the horns allowed for easier characterization of the lens. The theoretical radiation pattern of each horn, at the center frequency, is shown in Figs. 4 and 5. Gain values at the various test frequencies are shown in Table 1. Due to schedule constraints, the theoretically predicted gain values of the horns (see Table 1), rather than measured values, were used in determining the layered-lens performance (i.e., efficiency). This could be done because the software used to design the horns has been rigorously verified on a previous project and was found to be accurate within the measurement uncertainty. However, to ensure that no significant manufacturing problems occurred, the gain of the

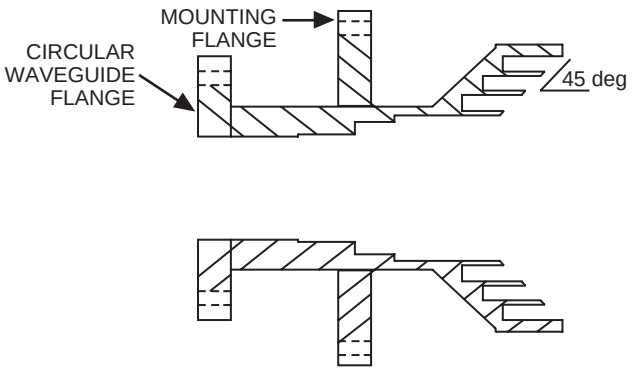

Fig. 3. Corrugated feed-horn representative cross section.

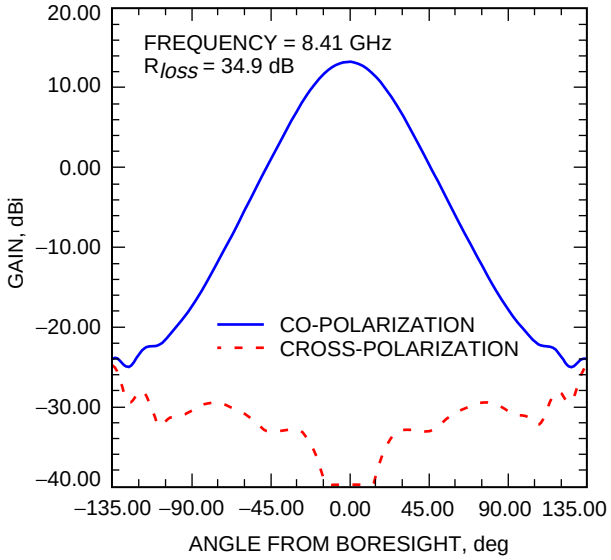

Fig. 4. X-band corrugated-horn theoretical performance (45-deg cut).

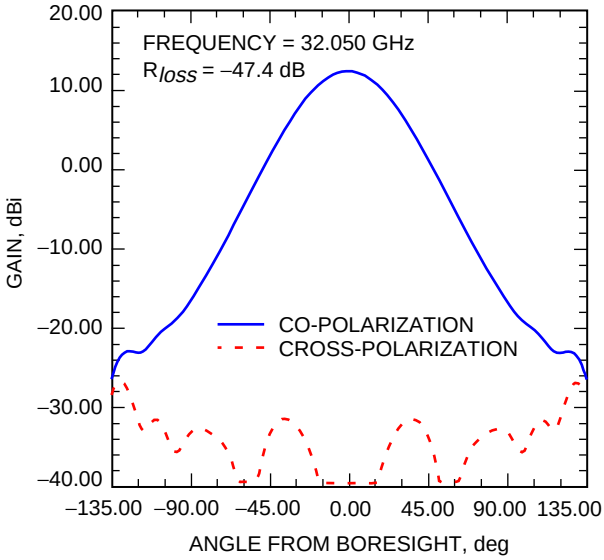

Fig. 5. Ka-band corrugated-horn theoretical performance (45-deg cut).

Ka-band horns was verified at 32.05 GHz. The gain was found to correlate extremely well with the theoretical value (i.e., the measured and theoretical value agreed within 0.1 dB). Both the X-band and the Ka-band horns were inspected after manufacturing, and no discrepancies were reported. Given this fact, it was felt that not measuring the X-band horns was a minor risk and allowed for more test time.

Before the design of the lens could be finalized, the program developed needed to be verified against measured results. Verification of the code was done using two separate single-layer arrays of identical elements designed to be resonant at 8.421 and 32.05 GHz, respectively. This single-layer configuration is hereafter referred to as the "equiphase" layer. The array elements were arranged to form a 610-mm circular array. Each equiphase layer was measured separately, and the results were compared with the data from the "infinite array" analysis. The dimensions and shapes of the elements used in the X-band and Ka-band equiphase layers can be seen in Table 2 and Fig. 6, respectively, where CL is the length of the dipole arms, EL is the length of the cross members of the dipole arms, and W is the width of the elements (see Fig. 6).

Table 1. X-band and Ka-band test-horn theoretical gain.

Frequency, GHz	Gain, dBi	Return loss, dB
8.121	13.10	−31.7
8.221	13.13	−32.7
8.321	13.17	−33.8
8.421	13.20	−34.9
8.521	13.23	−36.1
8.621	13.25	−37.8
8.721	13.26	−39.8
31.250	12.33	−31.5
31.650	12.31	−37.9
32.050	12.40	−47.3
32.450	12.48	−44.7
32.850	12.55	−39.7

Table 2. X-band and Ka-band equiphase element dimensions.

Band	CL, mm	EL, mm	W, mm
X-band	9.737	4.869	0.811
Ka-band	2.363	1.182	0.197

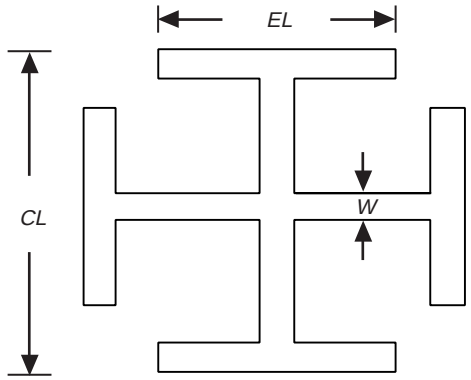

Fig. 6. Equiphase element geometry.

Copper-clad 0.5-oz (17.5-μm-thick) Rogers Corp. Ultralam® 1217 material was used to make all the layers. The equiphase layers were manufactured and tested using the specially designed horns and a Hewlett Packard 8510 Automatic Network Analyzer (see Fig. 7). The magnitude and phase of the transmitted (S_{21}) signal was measured.

When the layers were inspected after etching of the membranes, the dimensions of the crosses were found to be smaller than specified (i.e., the elements were over-etched). The measured results, after

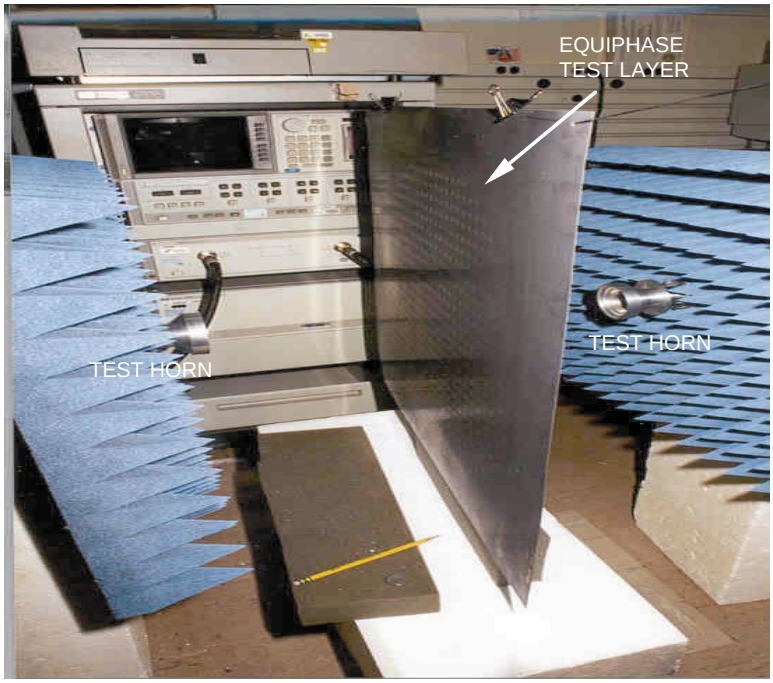

Fig. 7. Test setup used in S_{21} measurements of the single X-band equiphase layer.

accounting for the errors in the etching process, matched the theoretical predictions extremely closely, as can be seen from Figs. 8 and 9. Having validated the software, the design of the layered lens could then proceed. As previously mentioned, to assist in the diagnosis of any problems in the Ka-band three-layer lens, the X-band layered lens was also developed. The X-band unit allowed further verification of the software, along with the manufacturing process effects and material properties. This is because at a lower frequency the impact of mechanical imperfections, ohmic and dielectric losses, and testing difficulties is minimized.

The X-band layered-lens design was centered at 8.421 GHz, while the Ka-band design was centered at 32.050 GHz. Both lenses were designed for 60 percent efficiency, with theoretical gains of 34.4 dBi for the X-band lens and 44.93 dBi for the Ka-band lens. The spacing, S (see Fig. 1), between the layers of the lens is 8.406 mm and 1.819 mm for the X-band and Ka-band implementations.

III. Demonstration Hardware Performance Verification

The X-band testing was performed on an outdoor test range, as shown in Fig. 10, using a Scientific Atlanta Receiver 1783 and a Wiltron Synthesizer model 6769B as the transmitter. Patterns were taken at a distance of 23.62 m, R_1, between the lens and the transmitting antenna, which is in the far zone of the X-band lens ($2D^2/\lambda = 20.89$ m). The antenna was measured and data were collected for co- and cross-polarization (co-pol and cx-pol) for the E-, D-, and H-planes (i.e., $\phi = 0$, 45, and 90 deg cuts, respectively). Although the lens is not a body of revolution, it was found that the D-plane provides an average pattern for the lens (Fig. 11). For this reason, the D-planes are provided in this article for most of the patterns shown. Figure 12 shows a comparison between measured and theoretical performance.

The gain of the lens was determined by comparing the power received by the lens at a distance R_1 with the power received by the test horn at a distance $R_2 = 10.0$ m and compensating for the change in distance. Two different distances had to be used to minimize excessive receiver noise from the measurement due to

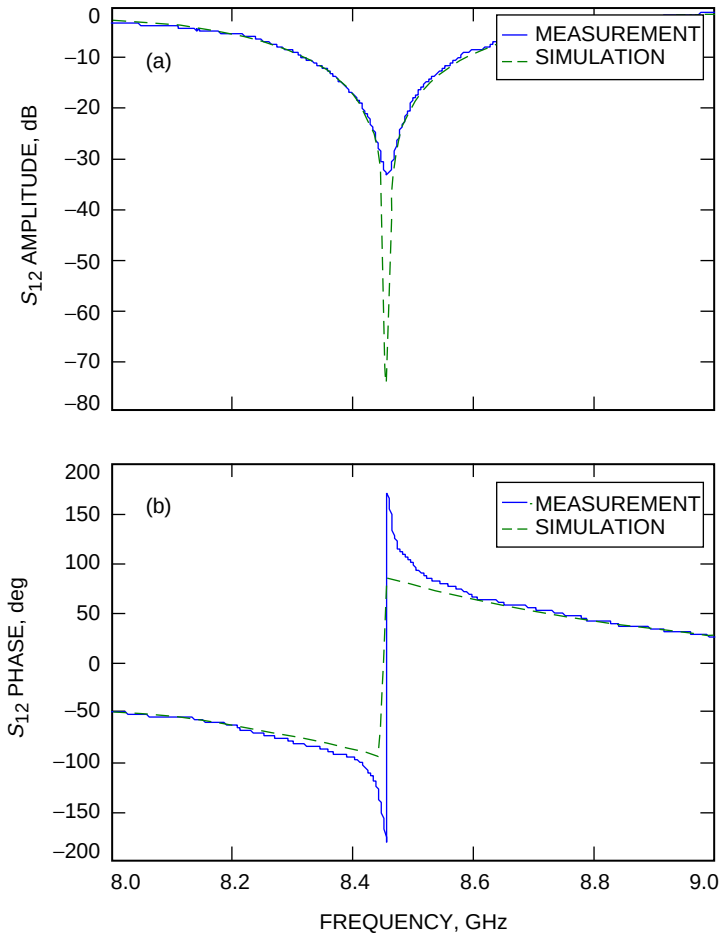

Fig. 8. Calculated and measured S_{12} software validation results for the single X-band equiphase layer: (a) amplitude and (b) phase.

the difference in gain between the horn and the lens. The layered-lens gain, G, is computed using Friis' equation:

$$P_R(\text{dBm}) = P_T(\text{dBm}) + G_T(\text{dBi}) + G_{AU}(\text{dBi}) - 20\log\left(\frac{4\pi R_x}{\lambda}\right)$$

where $P_R(\text{dBm})$ is the power received by the antenna under test, $P_T(\text{dBm})$ is the power transmitted from the source antenna (this is kept constant), $G_T(\text{dBi})$ is the gain of the transmitter antenna (this is also a constant), $G_{AU}(\text{dBi})$ is the gain of the antenna under test, R_x is the distance between the transmit and receive antennas, and λ is the free-space wavelength. Therefore, there is one equation for the lens and one for the horn measurements. Taking the difference between these two equations and rearranging the resulting equation, one obtains the lens gain as

$$G_{\text{lens}}(\text{dBi}) = G_{\text{horn}}(\text{dBi}) - \Delta P_R(\text{dB}) - 20\log\left(\frac{R_2}{R_1}\right)$$

where $\Delta P_R(\text{dB}) = P_{R-\text{horn}}(\text{dBm}) - P_{T-\text{lens}}(\text{dBm})$.

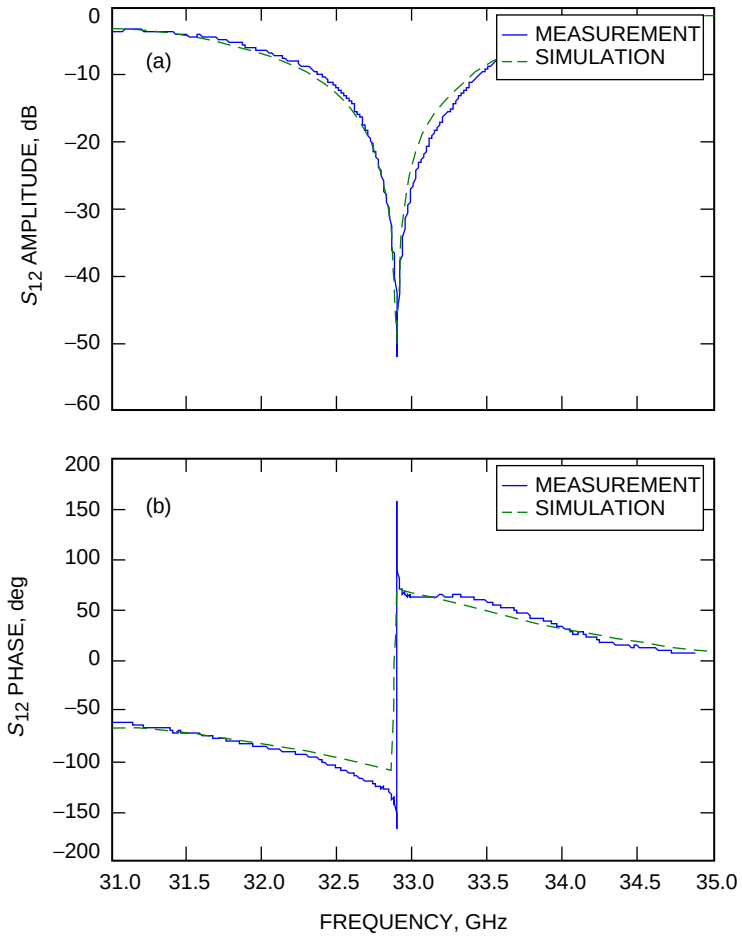

Fig. 9. Calculated and measured S_{12} software validation results for the single Ka-band equiphase layer: (a) amplitude and (b) phase.

From the measured gain of the lens (obtained from the above equation) and the maximum theoretical gain of the corresponding aperture, the aperture efficiency, eff, of the lens antenna can be obtained:

$$eff = \frac{G}{\left(\frac{\pi D}{\lambda}\right)^2}$$

To determine the lens' useful bandwidth, the gain of the X-band lens was measured over several frequencies, with the results as shown in Table 3. The measured radiation patterns can be seen in Fig. 13. The reason for the nonsymmetric data set relative to the 8.421-GHz center frequency is that the transitions that were used were found to over-mode at 8.6 GHz.

The Ka-band lens was measured using a similar setup on a different outdoor test range, as shown in Fig. 14. The far zone of the Ka-band lens starts at approximately 77.1 m. This distance is substantial, and the ranges that are available at the Jet Propulsion Laboratory (JPL) are substantially larger than 400 m. However, in antenna measurements it is best to use the smallest range that will meet the $2D^2/\lambda$ criterion, to avoid range reflections, and to have sufficient transmit power to assure a good signal-to-noise ratio. On a 400-m range, the available RF power would not have been sufficient to yield a good

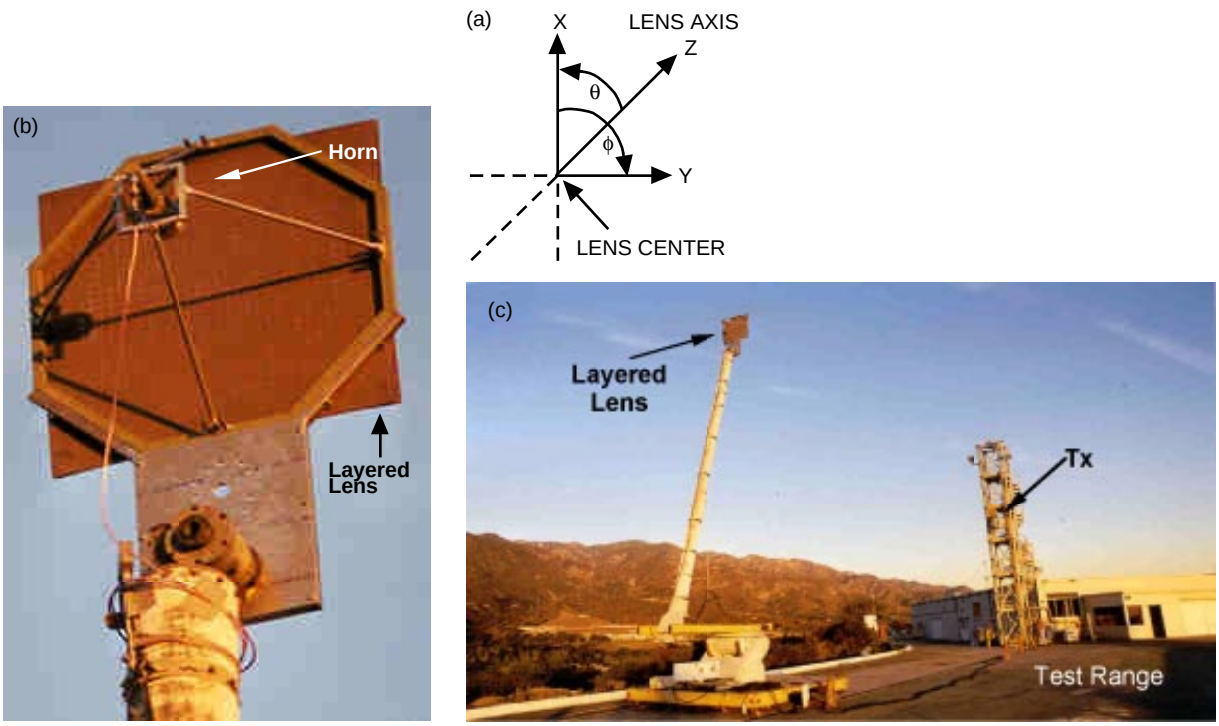

Fig. 10. X-band layered-lens test setup: (a) antenna coordinate system, (b) back view, and (c) test range.

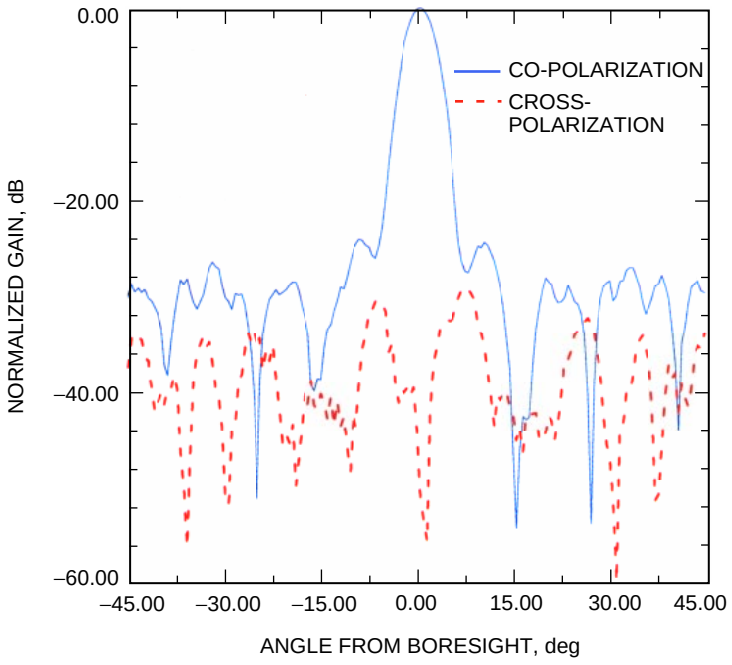

Fig. 11. X-band layered-lens measured co- and cross-polarization, D-cut (ϕ = 45 deg).

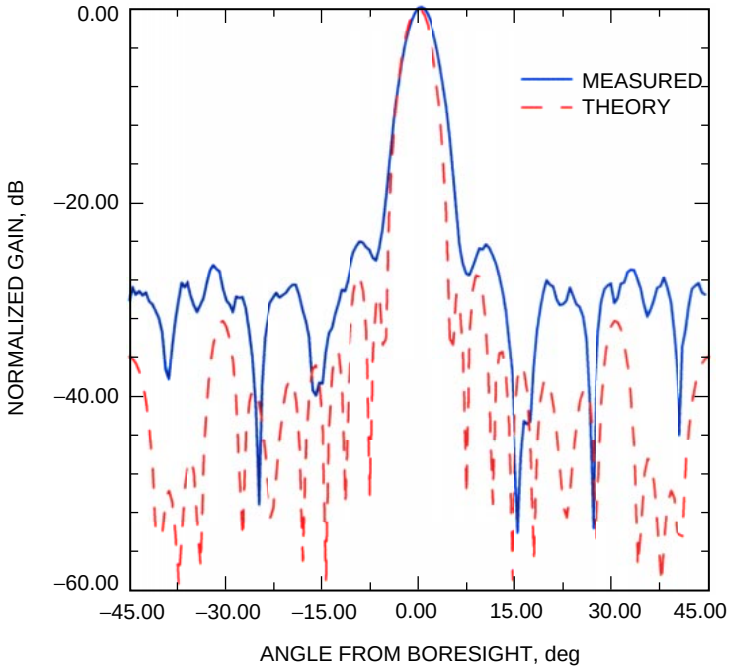

Fig. 12. X-band layered-lens co-polarization patterns, D-cut (ϕ = 45 deg).

Table 3. X-band three-layer lens gain and efficiency measured values.

Frequency, GHz	Theoretical gain, dBi	Measured gain, dBi	eff, percent
8.121	34.30	29.71	34.8
8.221	34.40	30.30	38.9
8.321	34.51	30.18	36.9
8.421	34.61	30.64	40.1
8.521	34.72	30.15	34.9

signal-to-noise ratio. Also, the 400-m range did not have a high-gain source antenna (>50 dBi), as required to minimize range reflections and yield accurate measurements. Accurate gain measurements also require good alignment, and alignment is time consuming on a 400-m range. Thus, measurements in any of the JPL longer ranges, without spending a considerable amount of time and effort, would not have yielded accurate measurements. Therefore, a decision was made to measure the antenna on a shorter range ($R_1 \approx 12.2$ m) using a focusing technique to compensate for the shorter range. The lens was focused to bring the far zone in—a technique akin to what one does with a photographic camera to sharpen the image when changing the focus from far out to close in [3,4]. Using an established reflector code, the performance of a reflector of equal gain was verified at 12.2 m after refocusing. The result was a slightly lower gain value (see Appendix B). This simulation gave an unrecovered gain loss of approximately 0.16 dB, which was added to the layered-lens gain measurement. As previously described, the gain of

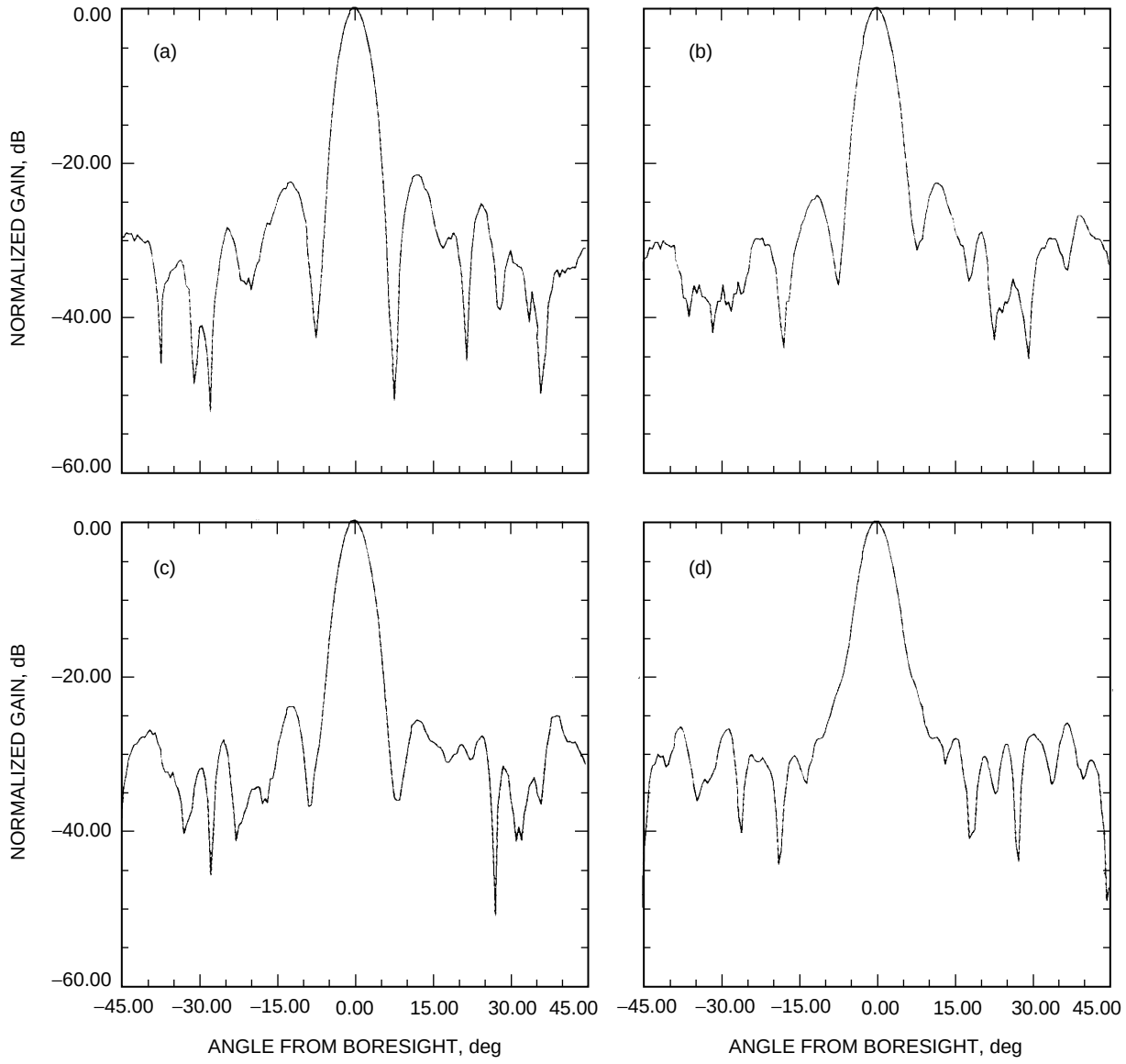

Fig. 13. X-band layered-lens patterns for (a) 8.121 GHz, (b) 8.221 GHz, (c) 8.321 GHz, and (d) 8.521 GHz.

the lens was determined by comparing the power received by the lens at a distance R_1 with the power received with the test horn at 3.05 m, R_2, and correcting for the change in distance. The gain of the lens at the center frequency was measured, and the layered-lens' co- and cross-polarization patterns were taken at 45 deg (see Figs. 15 and 16). To determine the lens bandwidth, its gain was also measured at several other frequencies (see Table 4). H-plane patterns were also taken (see Fig. 17). The associated measurement error on the antenna gain is ±0.6 dB for X-band and ±0.5 dB for Ka-band. The Ka-band lens measured gain and associated efficiency values are provided in Table 4. The return losses of the X-band and Ka-band lenses and the horns are sufficiently low to allow the mismatch contribution to the measurement error to be neglected (see Figs. 18 through 21).

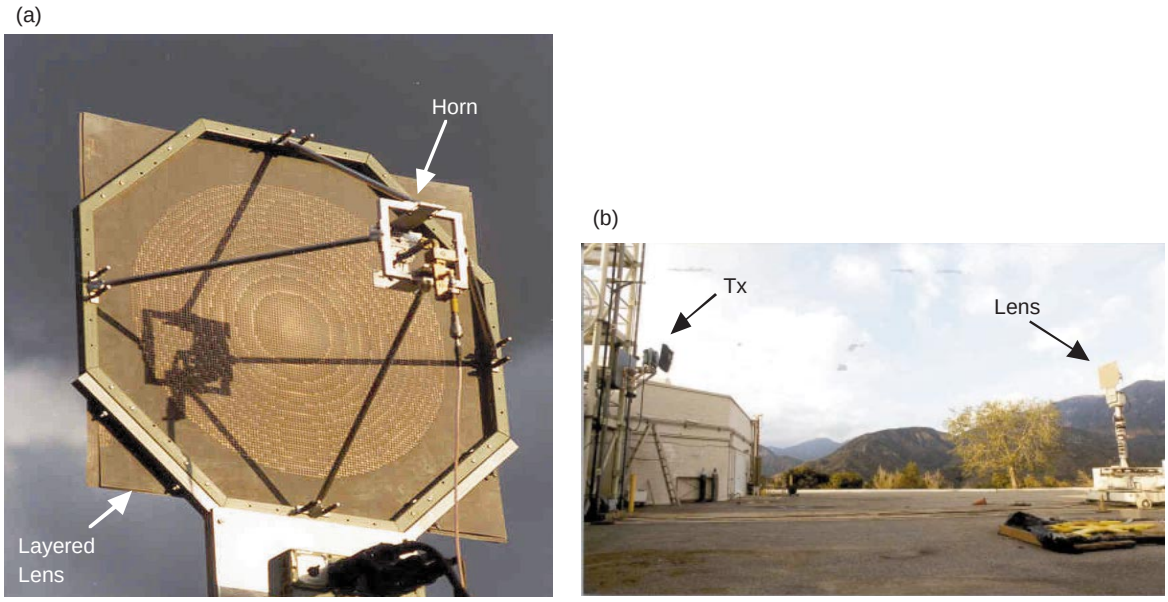

Fig. 14. Ka-band layered-lens test setup: (a) back view and (b) test range.

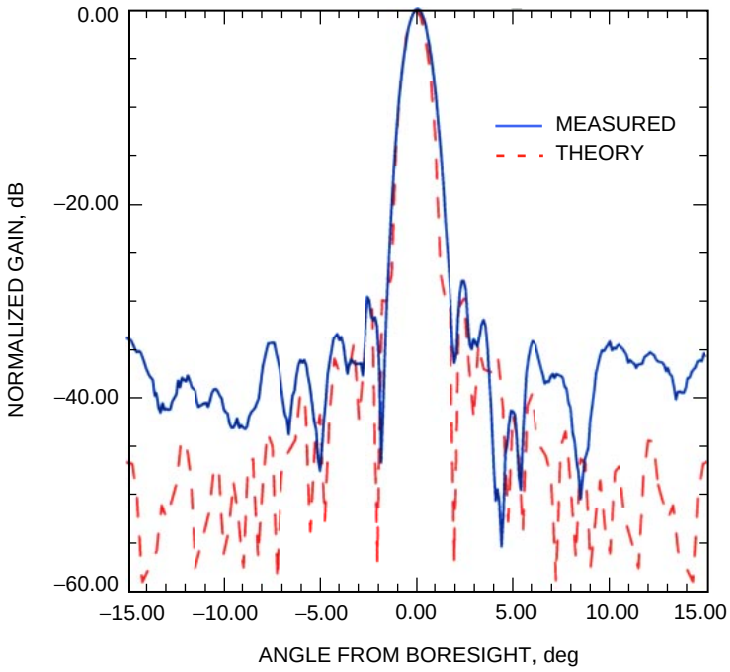

Fig. 15. Ka-band layered-lens co-polarization patterns, D-cut (ϕ = 45 deg).

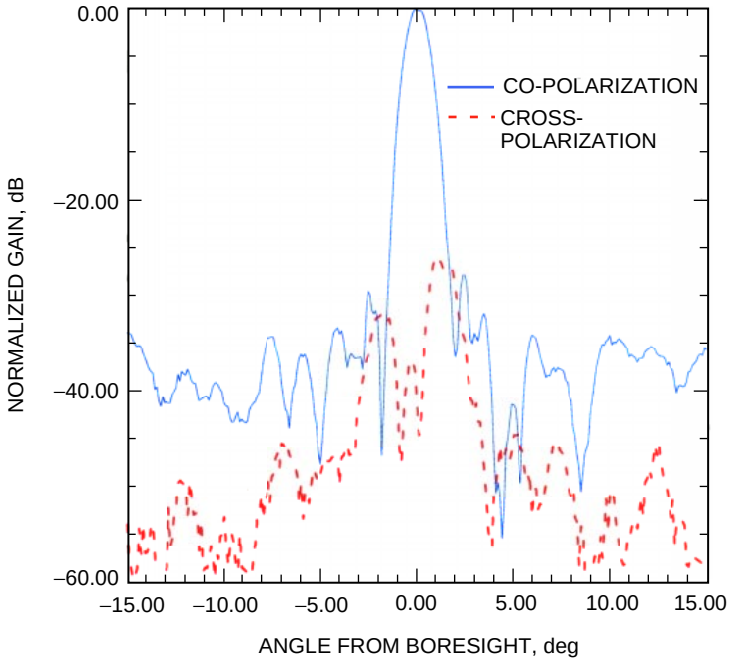

Fig. 16. Ka-band layered-lens measured co- and cross-polarization, D-cut (ϕ = 45 deg).

Table 4. Ka-band three-layer lens gain and efficiency measured values.

Frequency, GHz	Theoretical gain, dBi	Measured gain, dBi	eff, percent
31.450	46.06	40.08	25.6
31.650	46.11	40.99	30.7
32.050	46.22	41.39	33.0
32.450	46.33	40.79	27.9
32.850	46.44	39.33	19.5

IV. Conclusions

The purpose of this work was to demonstrate the feasibility of a three-layer lens for use with inflatable antenna technology. This work also successfully demonstrated the capability of JPL to design, build, and test such an antenna. Because the measured efficiency was lower than expected, further investigation is required to understand where efficiency is being lost. However, due to financial constraints, we were unable to perform a thorough investigation to determine the cause of the lower efficiency. It is believed that a layered-lens type of antenna can provide efficiencies greater than 50 percent. It is expected that a future study will yield the necessary improvement of the antenna efficiency. Layered lenses with antenna efficiencies >50 percent, and with their insensitivity to surface deformation (see Appendix A), are an excellent candidate for inflatable technology.

References

[1] S. Datthanasombat, A. Prata, Jr., L. R. Amaro, J. A. Harrell, S. Spitz, and J. Peret, "Layered Lens Antennas," IEEE AP-S International Symposium, Boston, Massachusetts, July 8–13, 2001.

[2] R. Milne, "Dipole Array Lens Antenna," *IEEE Transactions on Antennas and Propagation*, vol. AP-30, no. 4, pp. 704–712, July 1982.

[3] D. K. Cheng, "On the Simulation of Fraunhofer Radiation Patterns in the Fresnel Region," *IRE Transactions on Antennas and Propagation*, vol. AP-5, pp. 399–402, October 1957.

[4] T. S. Chu, "A Note on Simulating Fraunhofer Radiation Patterns in the Fresnel Region," *IEEE Transactions on Antennas and Propagation*, vol. AP-19, pp. 691–692, September 1971.

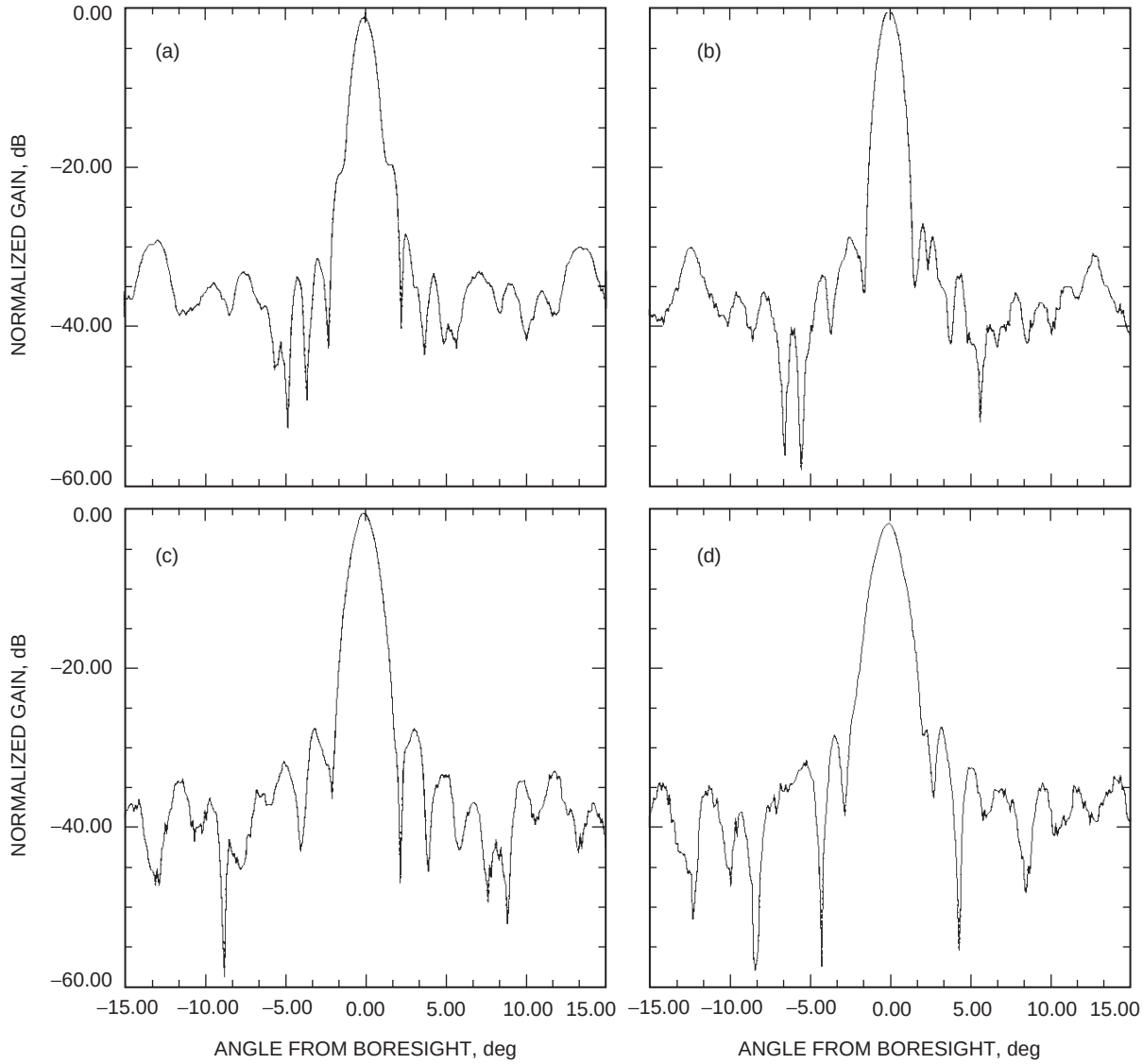

Fig. 17. Measured Ka-band layered-lens patterns for (a) 31.250 GHz, (b) 31.650 GHz, (c) 32.450 GHz, and (d) 32.850 GHz.

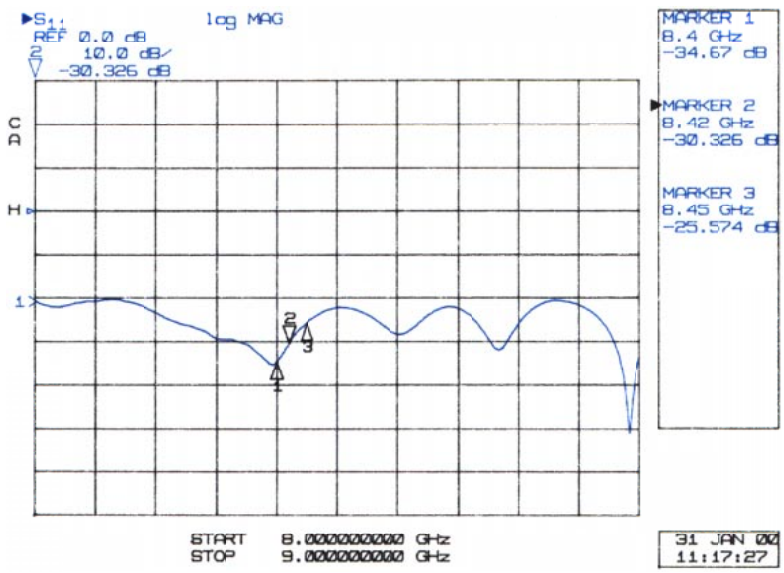

Fig. 18. X-band layered-lens return-loss measurement.

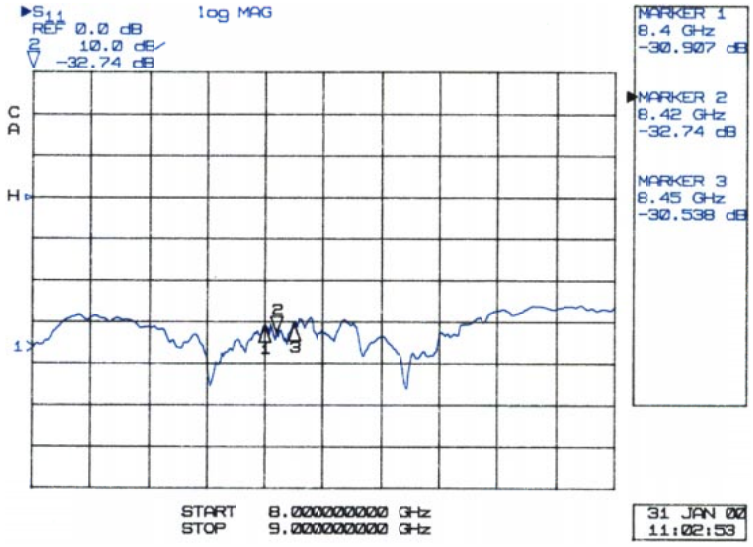

Fig. 19. X-band test-horn return-loss measurement.

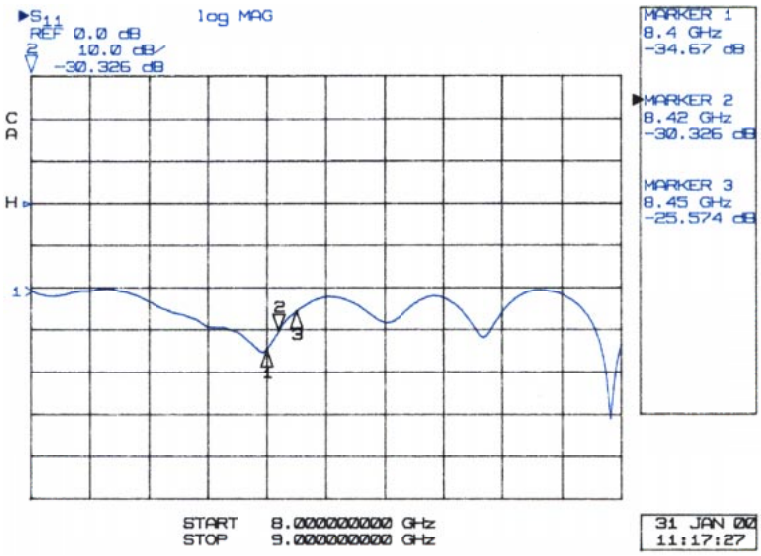

Fig. 20. Ka-band layered-lens return-loss measurement.

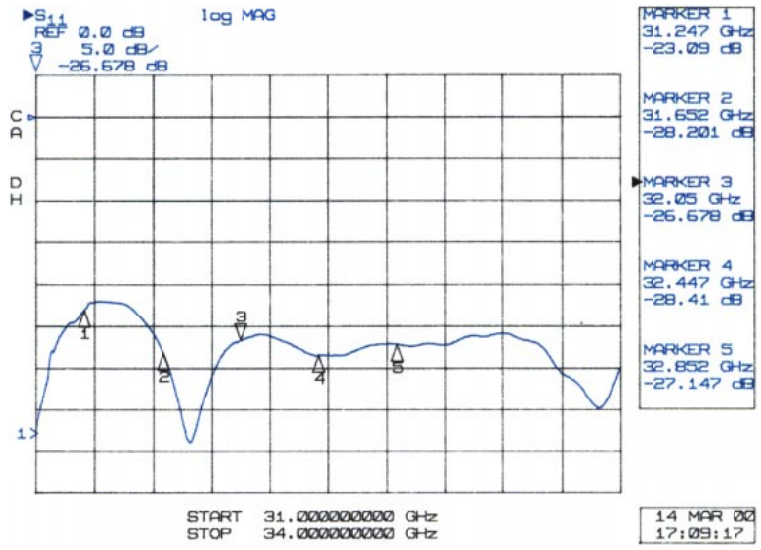

Fig. 21. Ka-band test-horn return-loss measurement.

Appendix A

Layered-Lens Dimensional Sensitivity

A surface distortion of magnitude δ will cause a phase error on the emerging wave at the aperture plane of both the lens and the reflector. The phase error in the lens is related to the path-length difference, Δ_l, incurred and can be seen from Fig. A-1 to be equal to

$$\Delta_l = OA - OB \cong \delta \left[\left(\frac{1}{\cos\theta} \right) - 1 \right]$$

Similarly, a surface distortion on the reflector will cause an error related to the path length, Δ_l, that can be seen from Fig. A-2 to be equal to

$$\Delta_\rho = OA - OB \cong \delta \left[1 + \left(\frac{1}{\cos\theta} \right) \right]$$

From these two equations, Table A-1 was constructed. The angular range of θ is from 0 to 60 deg since $\theta = 60$ deg would correspond to an F/D of less than 0.3 (an almost impractical F/D ratio). From the table it can be seen that the sensitivity of a reflector to surface deformations can be more than an order of magnitude larger than that of a lens.

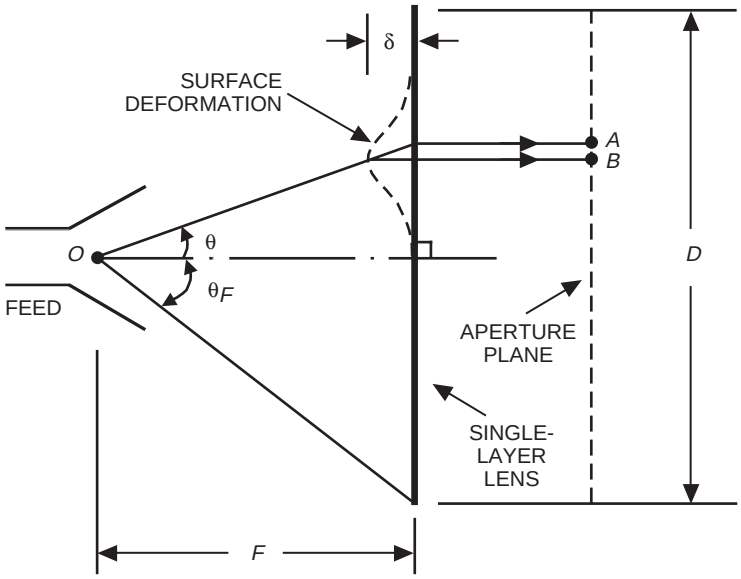

Fig. A-1. Surface distortion of magnitude δ on a single-layer lens.

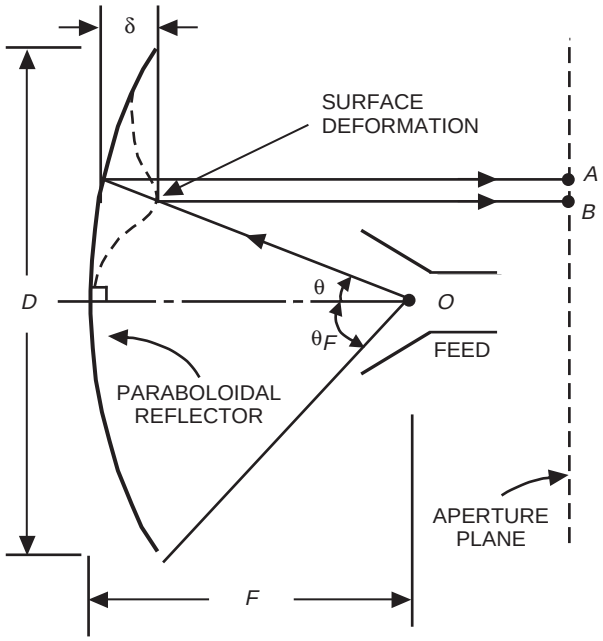

Fig. A-2. Surface distortion of magnitude δ on a paraboloidal reflector.

Table A-1. Associated errors for a lens and reflector surface.

θ, deg	Δ_l (lens)	Δ_ρ (reflector)
0	0.00δ	2.00δ
30	0.16δ	2.16δ
45	0.41δ	2.41δ
60	1.00δ	3.00δ

Appendix B

Measurement of Far-Zone Patterns of Collimating Apertures in the Near Zone

A useful technique for measuring the far zone (Fraunhofer zone) of collimating apertures in the near zone (Fresnel zone) has been demonstrated by several authors [1,2]. The geometrical relationships present in the measurement of a lens antenna are given in Eqs. (B-1) through (B-3) (the results shown in these equations are also valid for a focal-fed reflector system). The far- and near-zone arrangements are shown in Figs. B-1 and B-2, respectively.

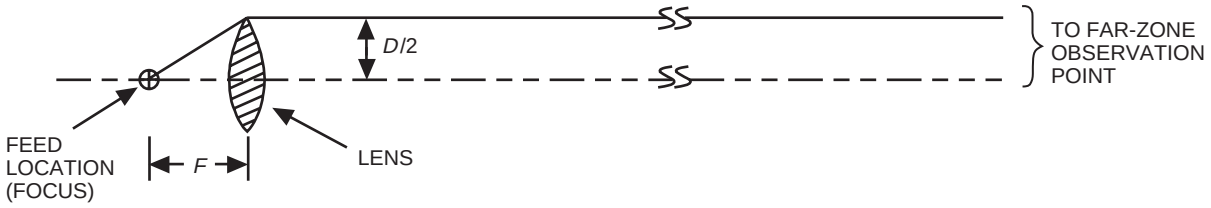

Fig. B-1. Lens arrangement with feed at focal point, base case.

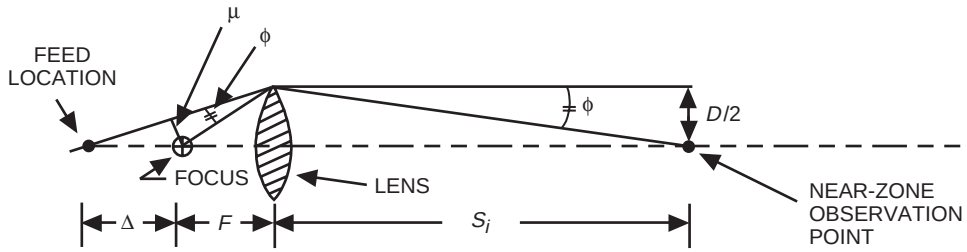

Fig. B-2. Lens arrangement with feed shifted from focal point, defocused case.

If the feed from Fig. B-1 is moved a distance, Δ, from the focal point to focus the lens at a near-zone observation point (as shown in Fig. B-2), and assuming that $\Delta << S_i$ and $\Delta << F$, then

$$\frac{D/2}{S_1} \approx \frac{\mu}{F} \tag{B-1}$$

$$\frac{D/2}{F} \approx \frac{\mu}{\Delta} \tag{B-2}$$

Dividing Eq. (B-1) by Eq. (B-2),

$$\frac{F}{S_i} \approx \frac{\Delta}{F}$$

Therefore,

$$\Delta \approx \frac{F^2}{S_i} \tag{B-3}$$

For example, if the following values are used for the lens,

$$S_i = 13.72 \text{ m}$$

$$D = 600 \text{ mm}$$

$$F = 305 \text{ mm}$$

then $\Delta = 6.80$ mm.

To test the quality of the approximation provided by Eq. (B-3), a physical optics program was used to obtain the far-zone pattern and gain for a paraboloidal reflector ($D = 610$ mm and $F = 305$ mm) in both the focused and the defocused cases. This was done for two frequencies, 8.425 and 32.05 GHz. The results obtained are given in Figs. B-3 through B-10. It can be seen from the 8.425-GHz results that the difference between the far-zone gain and the gain at S_i is 0.26 dB (see Figs. B-3 and B-4). Changing the position of the feed by moving 6.80 mm away from the focus (i.e., defocusing) reduces the error in gain to 0.10 dB (see Figs. B-3 and B-5). By further adjusting the feed location to 8.00 mm from the focus, an additional 0.02-dB improvement was obtained (see Figs. B-3 and B-6). Using the value of 6.80 mm (e.g., the value obtained from optics) causes a 0.03-dB error, which is negligible. The same process was followed for a frequency of 32.05 GHz. The difference between the far-zone gain and the gain calculated at S_i is 1.91 dB, which is quite large (see Figs. B-7 and B-8). When the feed is moved 6.80 mm away from the focus, all but 0.16 dB of the far-zone gain is recovered (see Figs. B-7 and B-9). A further adjustment of the feed ($\Delta = 8.00$ mm) recovers an additional 0.06 dB of the far-zone gain (see Figs. B-7 and B-10). The focus correction [Eq. (B-3)] gave reasonable results at 32 GHz also, even though substantial approximations were used in its derivation. These two cases demonstrate that a collimating aperture can be measured with reasonable accuracy in the near zone. To use this technique for measuring the gain of a reflector/lens antenna in the Fresnel region, after careful alignment of the antenna, one would adjust the antenna feed for maximum gain. The adjustment would ensure that the error in the measurement would be minimized to values similar to those mentioned above, as long as the antenna F/D is about 0.5 or greater and S_i is large relative to Δ.

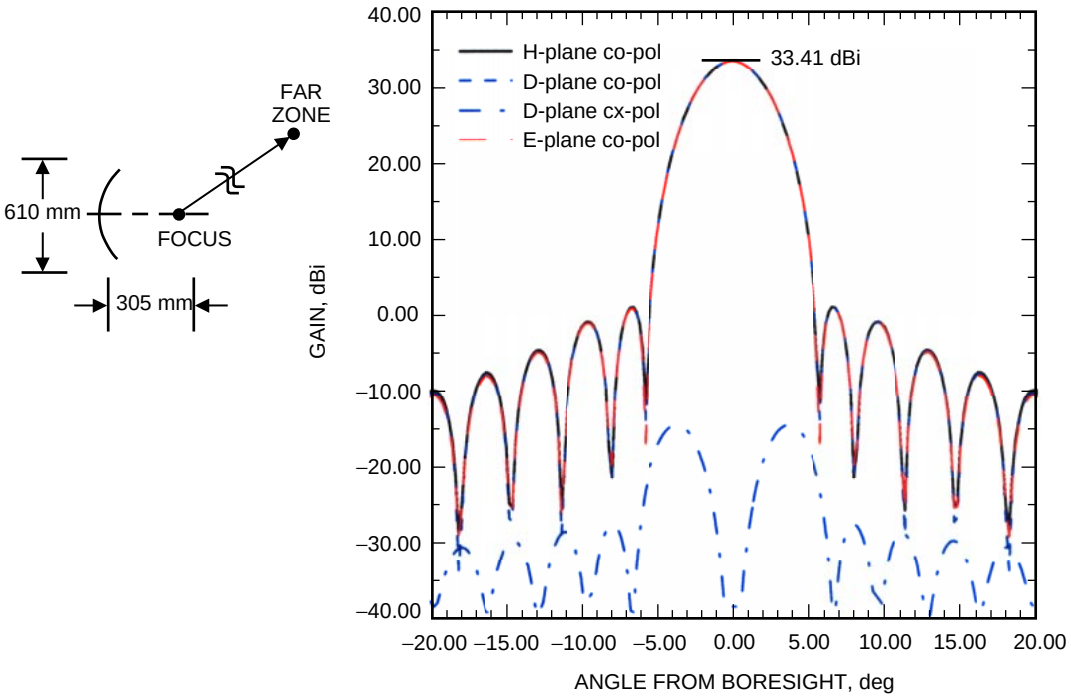

Fig. B-3. X-band antenna far-zone pattern and gain with feed located at focus.

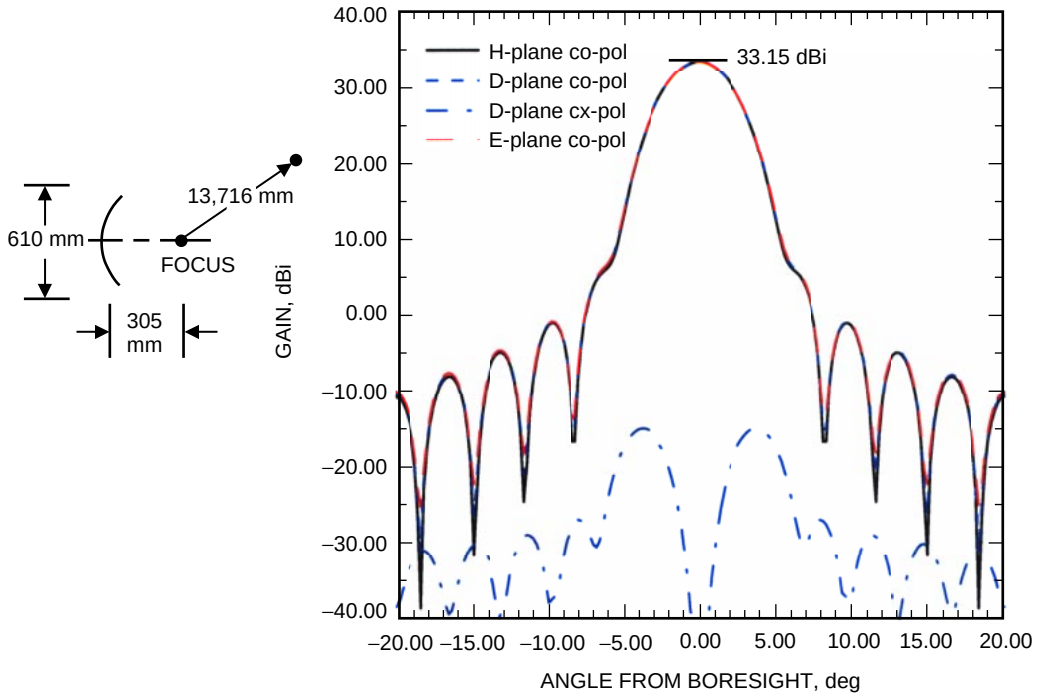

Fig. B-4. X-band antenna near-zone pattern and gain with feed located at focus.

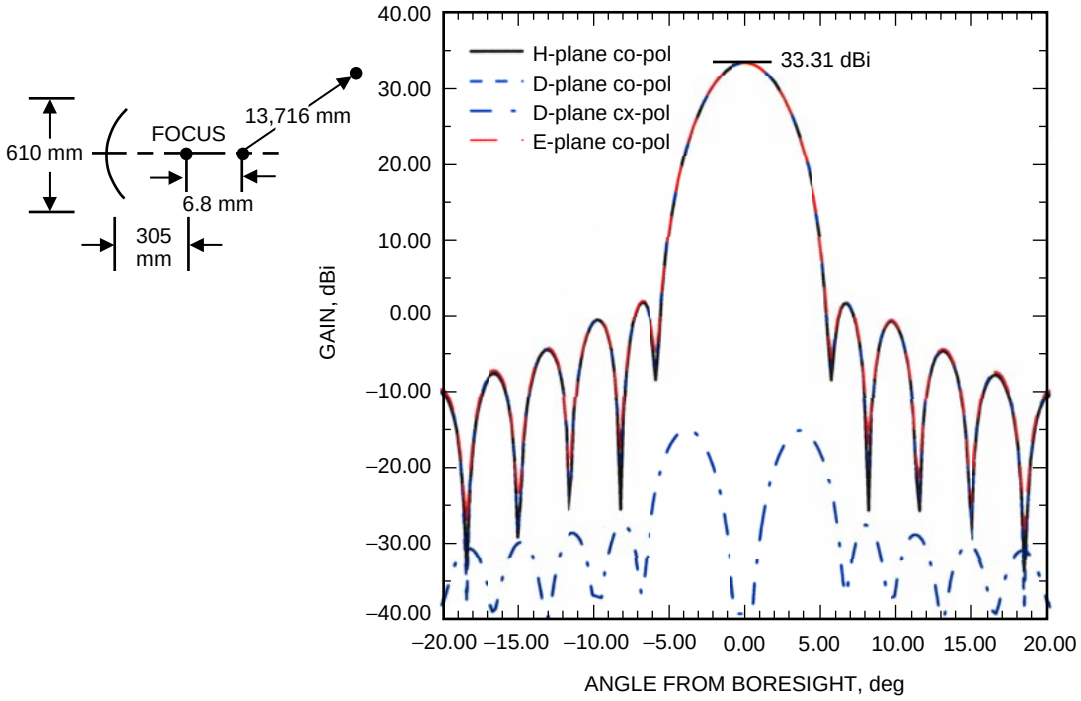

Fig. B-5. X-band antenna near-zone pattern and gain with feed located 6.80 mm from focus.

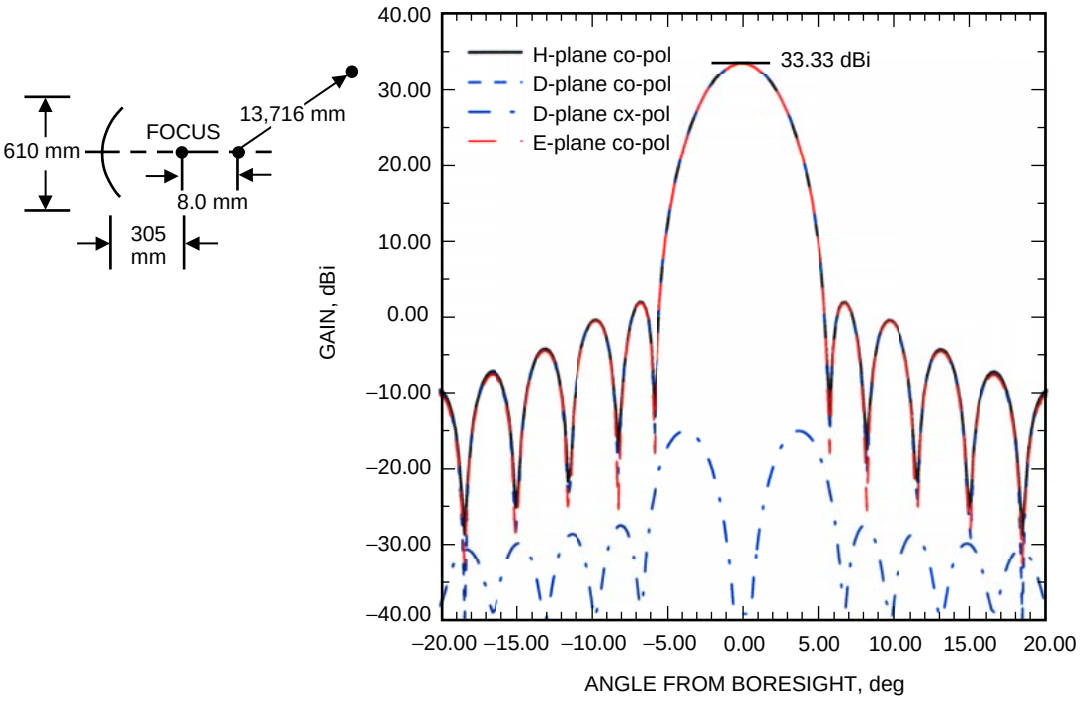

Fig. B-6. X-band antenna near-zone pattern and gain with feed located 8.00 mm from focus.

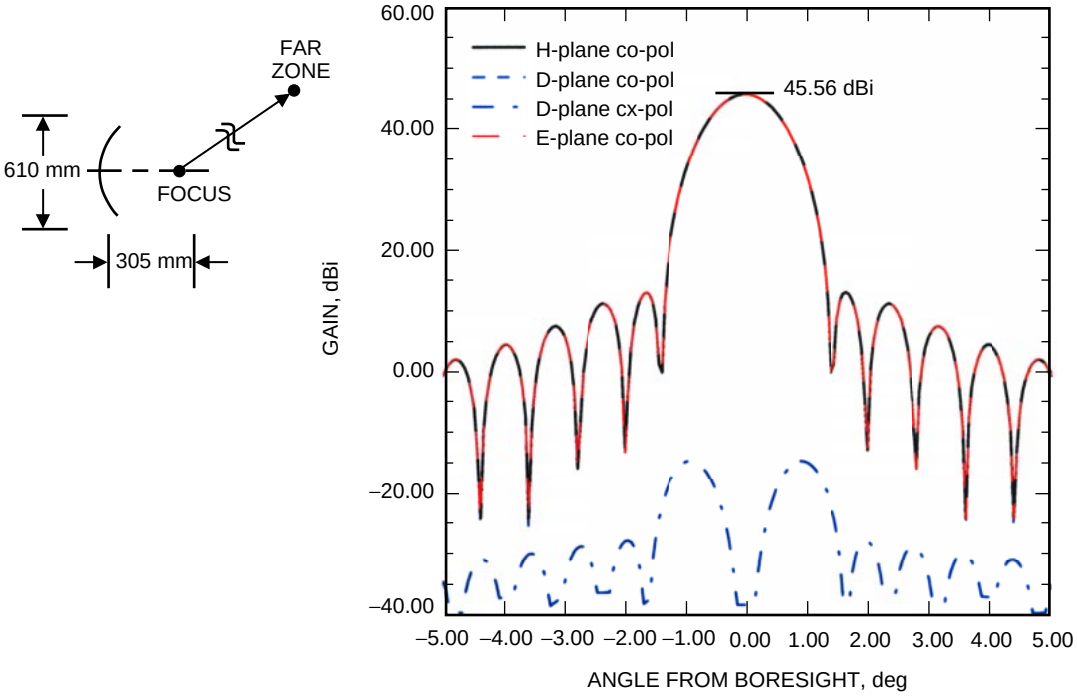

Fig. B-7. Ka-band antenna far-zone pattern and gain with feed located at focus.

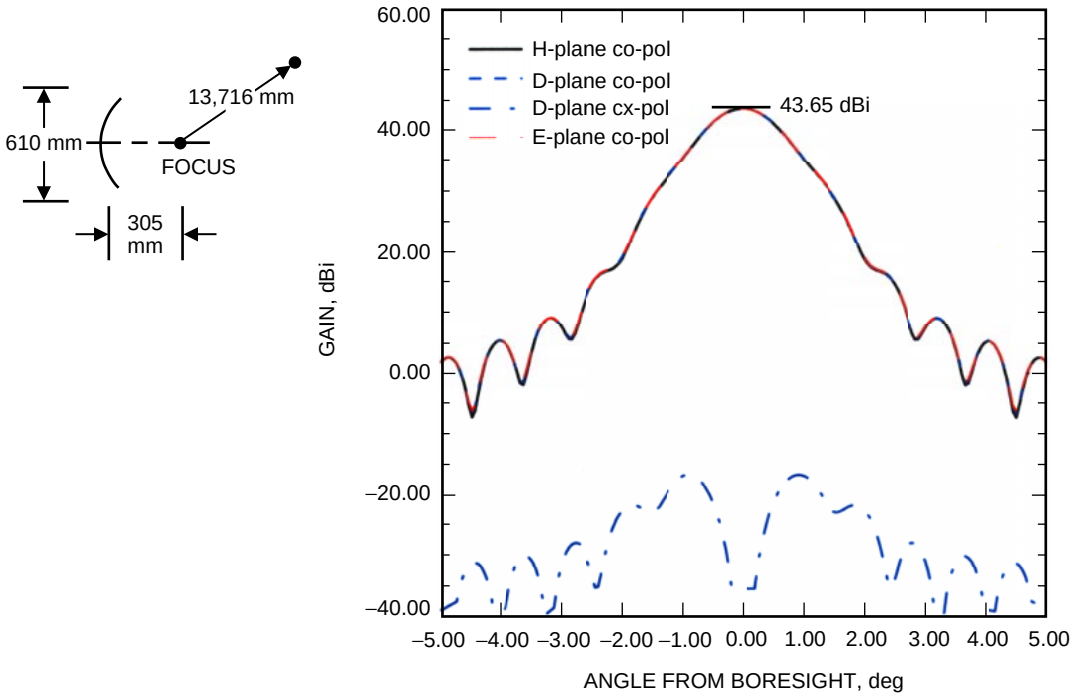

Fig. B-8. Ka-band antenna near-zone pattern and gain with feed located at focus.

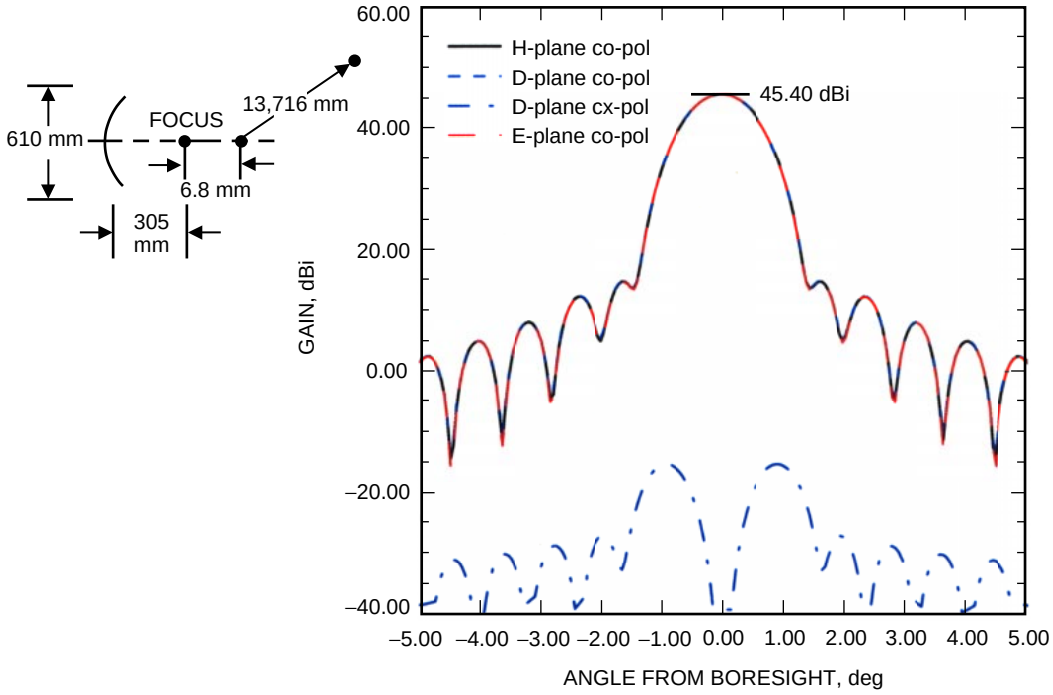

Fig. B-9. X-band antenna near-zone pattern and gain with feed located 6.80 mm from focus.

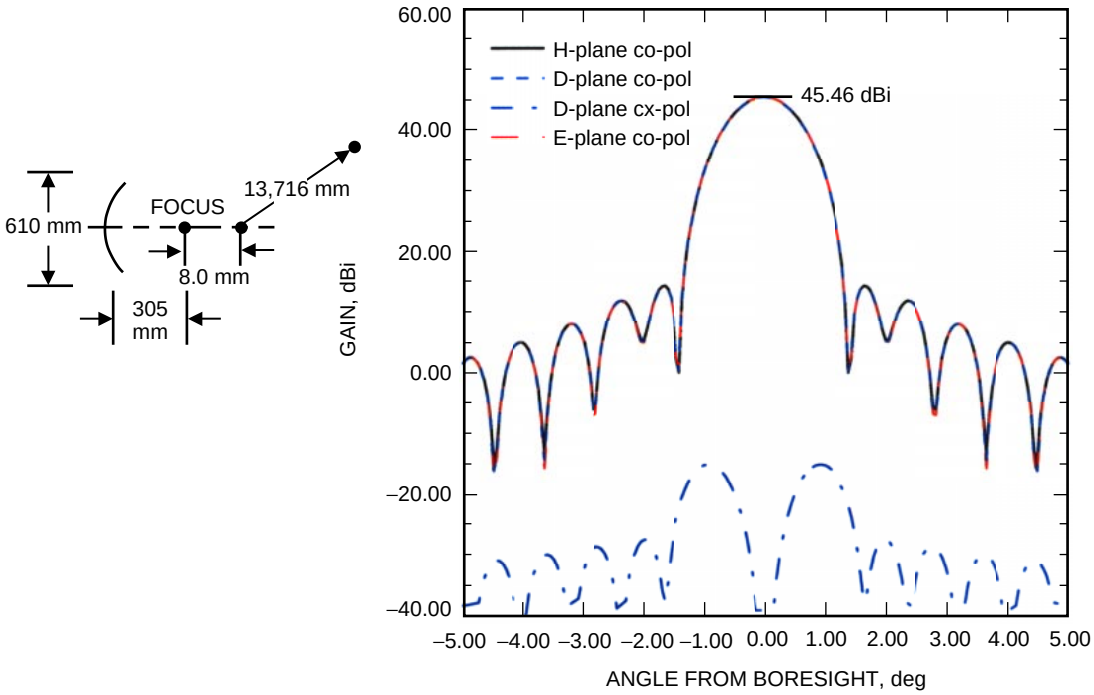

Fig. B-10. Ka-band antenna near-zone pattern and gain with feed located 8.00 mm from focus.